Development 139, 2604-2613 (2012) doi:10.1242/dev.077594

Sonic hedgehog is indirectly required for intraretinal axon pathfinding by regulating chemokine expression in the optic stalk

Cornelia Stacher Hörndli[1,2,*] and Chi-Bin Chien[1,2,3,‡]

SUMMARY

Successful axon pathfinding requires both correct patterning of tissues, which will later harbor axonal tracts, and precise localization of axon guidance cues along these tracts at the time of axon outgrowth. Retinal ganglion cell (RGC) axons grow towards the optic disc in the central retina, where they turn to exit the eye through the optic nerve. Normal patterning of the optic disc and stalk and the expression of guidance cues at this choice point are necessary for the exit of RGC axons out of the eye. Sonic hedgehog (Shh) has been implicated in both patterning of ocular tissue and direct guidance of RGC axons. Here, we examine the precise spatial and temporal requirement for Hedgehog (Hh) signaling for intraretinal axon pathfinding and show that Shh acts to pattern the optic stalk in zebrafish but does not guide RGC axons inside the eye directly. We further reveal an interaction between the Hh and chemokine pathways for axon guidance and show that *cxcl12a* functions downstream of Shh and depends on Shh for its expression at the optic disc. Together, our results support a model in which Shh acts in RGC axon pathfinding indirectly by regulating axon guidance cues at the optic disc through patterning of the optic stalk.

KEY WORDS: Axon guidance, Tissue patterning, Hh signaling, Shh, Cxcl12, Zebrafish

INTRODUCTION

The first steps for correct RGC axon pathfinding to the optic tectum are axon extension towards the optic disc and turning into the optic stalk to exit the eye through the optic nerve. When RGC axons fail to turn at the optic disc, they project within the eye and become trapped. Several molecules have been implicated in axon pathfinding out of the eye, acting either through ocular tissue patterning, direct axon guidance or modulation of guidance cues (Deiner et al., 1997; Schauerte et al., 1998; Dakubo et al., 2003; Li et al., 2005). Shh is one factor that regulates ocular patterning in multiple species. A gradient of Shh along the proximodistal axis, formed by *shh* expression in the floorplate and notochord, has been implicated in specifying early eye tissue into optic stalk and retina through regulation of Pax2 and Pax6 expression domains (Ekker et al., 1995; Macdonald et al., 1995; Perron et al., 2003). Additionally, Shh expressed by RGCs is required for normal formation of astrocytes at the optic disc and stalk in mouse, with subsequent effects on RGC axon guidance (Wallace and Raff, 1999; Dakubo et al., 2003; Dakubo et al., 2008). However, there is also evidence for direct axon guidance by Shh. Both in vitro and in vivo studies in mouse and chick have implicated Shh in RGC axon guidance by signaling through non-canonical Hh pathways independent of target gene transcription (Trousse et al., 2001; Kolpak et al., 2005; Kolpak et al., 2009; Sánchez-Camacho and Bovolenta, 2008; Fabre et al., 2010; Gordon et al., 2010).

In this study, we used zebrafish to determine whether Shh regulates intraretinal axon pathfinding indirectly through tissue patterning or directly as a guidance molecule. Our results strongly suggest an indirect requirement for Hh signaling in intraretinal pathfinding through patterning of the optic stalk and argue against a direct requirement for Shh in intraretinal axon guidance in zebrafish. We show further that Shh regulates the expression of several genes at the optic stalk and disc. One of these, *cxcl12a*, has previously been implicated in intraretinal axon guidance in zebrafish (Li et al., 2005). We show that the Hh and chemokine signaling pathways interact genetically for axon guidance out of the eye. Altogether, our data lead us to propose that Hh signaling during early optic vesicle development is required for proper optic stalk patterning and correct expression of downstream guidance molecules, specifically *cxcl12a*, at the optic disc that direct RGC axons out of the eye.

MATERIALS AND METHODS

Mutant and transgenic lines

Fish were of Tü or TL strains. Embryos were raised at 28.5°C in 0.1 mM phenylthiourea. Mutant alleles used were: *shha*^{tbx392} (Schauerte et al., 1998), *smo*^{hi1640Tg} (Chen et al., 2001), *cxcl12a*^{my054} (Valentin et al., 2007) and *cxcr4b* ^{t26035} (Knaut et al., 2003). Transgenic lines used were: *Tg(–17.6isl2b:GFP)*^{zc7} (Pittman et al., 2008), *Tg(–17.6isl2b:tagRFP)*^{zc80}, *Tg(hsp70l:GFP)*^{mik} and *Tg(hsp70l:cxcl12a-2A-EGFP)*^{zc85}.

The *Tg(hsp70l:cxcl12a-2A-EGFP)*^{zc85} line was generated using the Tol2kit (Kwan et al., 2007). The *cxcl12a* full-length middle clone was generated using primers with attB1F and attB2R sites flanking the *cxcl12a* coding sequence, omitting the stop codon.

In situ hybridization

Embryos were fixed in 4% paraformaldehyde (PFA) overnight at 4°C, washed in PBS, dehydrated through a methanol series and stored at –20°C. Whole-mount in situ hybridization staining was performed according to Thisse and Thisse (Thisse and Thisse, 2008). For sectioning, embryos were prepared as described previously (Pittman et al., 2008) and sectioned at 15 μm on a Reichert-Jung 2050 Supercut microtome with a glass knife. Images were taken on an Olympus BX51WI compound microscope using a SPOT RT3 camera. Images were processed using Adobe Photoshop CS2.

[1]Program in Neuroscience, [2]Department of Neurobiology and Anatomy, 401 MREB, and [3]Brain Institute, University of Utah Medical Center, 20 North 1900 East, Salt Lake City, UT 84132, USA.

*Author for correspondence (coni.horndli@neuro.utah.edu)
‡Deceased

Accepted 8 May 2012

Immunohistochemistry

For whole-mount immunohistochemistry, embryos were fixed (4% PFA, overnight), washed in PBS, dehydrated in methanol and stored at –20°C, then rehydrated and washed in PBST (PBS+0.1% Tween 20), permeabilized with 0.1% collagenase [15 minutes, room temperature (RT)]. Embryos were blocked (2 hours, RT) with 10% newborn calf serum with 0.1% Tween 20 (NCST), incubated in primary antibodies (overnight, 4°C), washed in PBST, incubated in secondary antibodies plus ToPro3 (1:1000, Invitrogen; 4 hours, RT) and washed in PBST. Primary antibodies used were: mouse anti-GFP (1:200, Millipore), rabbit anti-GFP (1:200, Invitrogen), mouse anti-tagRFP (1:200; Evrogen) and rabbit anti-Pax2a (1:300, gift of Dr Michael Brand, Center for Regenerative Therapies Dresden, Technische Universität Dresden, Germany). Secondary antibodies used were: goat anti-mouse 488 (1:200; Invitrogen), goat anti-rabbit 488 (1:200, Invitrogen), goat anti-mouse Cy3 (1:200, Jackson ImmunoResearch) and goat anti-rabbit Cy3 (1:200, Jackson ImmunoResearch).

Confocal microscopy

Embryos were cleared in 50% glycerol/H_2O (3 hours, 4°C) and stored at 4°C in 80% glycerol/H_2O. Heads were dissected and embedded between two #0 cover slips separated by two layers of black electrical tape. Images were taken on a FV1000-XY Olympus confocal microscope using a 40× water objective. Maximum-intensity projection images were generated using ImageJ (http://rsbweb.nih.gov/ij/index.html).

SANT75 treatment

Twenty *isl2b:GFP* embryos were incubated in 40 μM SANT75 (gift of Dr Shuo Lin, University of California Los Angeles, CA, USA) in 1% DMSO in E3 or E2/GN (E2+10 μg/ml gentamycin sulfate) bath-applied in 6-well plates. For the 1-24 hours post-fertilization (hpf) treatment, SANT75 was washed off with E3 (three 15 minute washes). Phenotypes were scored using an Olympus SZX16 fluorescence stereomicroscope. Embryos with stalled RGC wave progression and no visible axon outgrowth were not included in the analysis.

Cell transplants

Embryos were anesthetized with tricaine, mounted in 1% low-melting point (LMP) agarose and covered with fish ringer. Roughly 20 retinal precursors were transplanted at 24 hpf. For ectopic *cxcl12a* expression: *hsp70l:EGFP* or *hsp70l:cxcl12a-2A-EGFP* embryos were used as donors. *shha* or wild-type (wt) embryos were used as hosts. About 50 anterior retinal cells were transplanted at 24 hpf into the anterior eye of host embryos. Hosts and donors were subjected to three rounds of heat-shock (40°C) at 28, 32 and 36 hpf.

Morpholino injections

*ath5*MO (4 ng) was injected at the 1-cell stage as described previously (Pittman et al., 2008). Inhibition of RGC differentiation in morphants was monitored using *isl2b:GFP* embryos. Morphants were used as host embryos for transplant experiments as described above. *netrin1a*SBMO (5.6 ng) was co-injected with 2 ng *p53*MO (Langheinrich et al., 2002). *p53*MO morphants served as controls. Inhibition of *netrin1a* mRNA splicing was tested by RT-PCR (Wilson et al., 2006). *shhb*MO (formerly known as *twhh*; 2 ng) (Hammond et al., 2003) with 2 ng *p53*MO was injected at the 1-cell stage.

Focal lipophilic dye injections

DiI or DiO was injected as previously described (Poulain et al., 2010). Briefly, microinjection needles were coated with melted dye crystals. Needles were quickly inserted into RGC layer of fixed embryos embedded laterally in 1% LMP agarose. Dye was allowed to diffuse overnight (RT). Embryos were washed in PBS and cleared with glycerol for imaging.

Statistical analysis

Fisher's exact test was calculated using the VassarStats website (http://faculty.vassar.edu/lowry/fisher.html). Student's *t*-test was calculated using Microsoft Excel. For the Mann-Whitney U test, embryos from three experiments were pooled for each genotype and ranked into categories. The percentage of embryos with delayed or no RGC layer differentiation was equal for both phenotypes; these embryos were excluded from the final analysis. Embryos were scored at 2 days post-fertilization (dpf) using an Olympus SZX16 stereomicroscope. Statistical difference between the ranking of the two genotypes was calculated using Mann-Whitney U statistics on the VassarStats website (http://faculty.vassar.edu/lowry/utest.html).

RESULTS

Hh mutant RGC axons make intraretinal pathfinding errors

In wild-type (wt) zebrafish, RGC axons project towards the optic disc in the central retina and exit the eye through the optic nerve. RGCs and their projections were visualized using embryos carrying the *isl2b* transgene, which is expressed in RGCs and photoreceptors inside the eye and extra-retinal expression of which includes the trigeminal ganglion (Pittman et al., 2008) (Fig. 1A,D,G,I). In *sonic hedgehog a* (*shha*) mutants, many RGC axons fail to exit through the optic nerve and become trapped within the eye, projecting posteriorly or anteriorly within the retina (Fig. 1B,E,H,J). In addition, RGC axons that exit the eye through the optic nerve in *shha* mutants often make mistakes further along the pathway and project to the ipsilateral optic tectum instead of crossing at the chiasm (Fig. 1B). Hh pathway mutations lead to retinal cell proliferation defects (Neumann and Nuesslein-Volhard, 2000), which result in decreased eye size compared with wt (Fig. 1D-F).

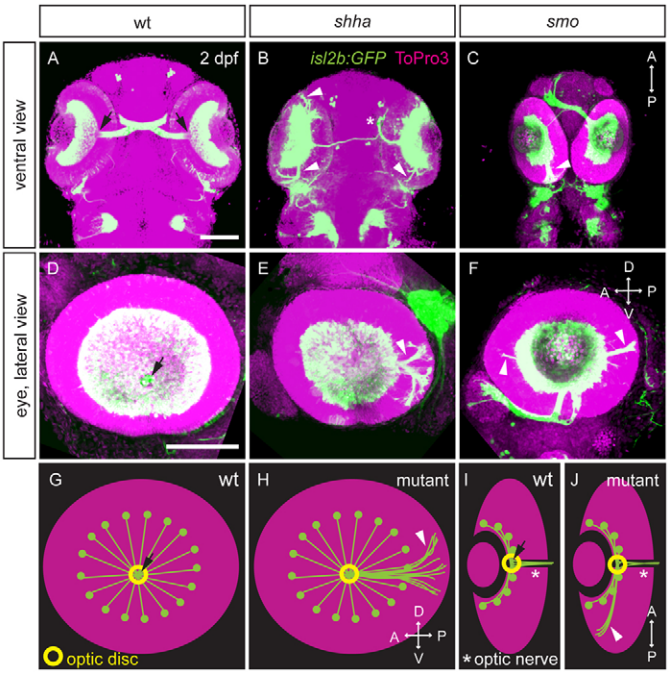

Fig. 1. Intraretinal axon pathfinding defects in Hh pathway mutants. (**A-J**) Retinal projections at 2 dpf in wt, *shha* and *smo* zebrafish embryos with *isl2b:GFP* (green) or *isl2b:tagRFP* (pseudocolored green in C,F) transgene; nuclei, ToPro3 (magenta). Ventral (A-C) or lateral views (D-F) of maximum-intensity projections and schematics of wt and mutant axon projections showing lateral (G,H) and ventral views (I,J) are shown. In wt embryos (A,D,G,I), RGC axons converge at the optic disc (arrow), where they turn and pass through the optic nerve (I, asterisk). In *shha* (B,E,H,J) and *smo* (C,F,H,J) mutants, some axons fail to exit the eye, projecting posteriorly or occasionally anteriorly within the eye (arrowheads). Hh mutants also exhibit misprojections to the ipsilateral optic tectum (asterisk in B). D, dorsal; V, ventral; A, anterior; P, posterior. Scale bars: 100 μm.

Zebrafish carry two paralogs of *shh*: *shha* and *shhb*. However, although both variants are expressed in RGCs (Neumann and Nuesslein-Volhard, 2000), only the loss of *shha* results in intraretinal pathfinding errors. Knockdown of *shhb* in wt embryos using a translation blocking morpholino (MO) did not induce intraretinal axon guidance errors, whereas MO injections into *shha* embryos led to severe midline patterning defects similar to *smo* mutants (Varga et al., 2001) without an increase in the severity of the intraretinal pathfinding phenotype (data not shown).

Focal lipophilic dye injections in the RGC layer revealed that RGC axons from all quadrants of the *shha* retina project towards the optic disc, where some axons fail to turn and misproject within the eye, with a predominance of posterior over anterior projections (supplementary material Fig. S1).

The ligand Shh binds to Patched (Ptch) receptors, which signal through Smoothened (Smo) to activate the Hh signaling pathway (Ingham and McMahon, 2001). Zebrafish carry one *smo* gene and mutations in *smo* therefore lead to complete inhibition of the Hh signaling pathway. *smo* embryos exhibit intraretinal guidance errors and ipsilateral projections analogous to those seen in *shha* mutants (Fig. 1C,F,H,J). *Smo* embryos show strong midline patterning defects, but are rescued from complete cyclopia by maternally expressed *smo* (Varga et al., 2001). In summary, Hh signaling is required for correct intraretinal axon pathfinding in zebrafish.

Hh pathway components are expressed during eye patterning and RGC axon outgrowth

To determine how Hh signaling regulates intraretinal axon pathfinding, we analyzed the spatial and temporal expression patterns of both ligand and receptor components. We performed in situ hybridization for *shha*, *ptch2* and *smo* at 16 hours post fertilization (hpf), after the optic vesicle has formed (Li et al., 2000), at 28 hpf, just as RGCs start to differentiate (Laessing and Stuermer, 1996), and at 48 hpf, when most RGCs have differentiated and several axons have reached the optic tectum (Laessing and Stuermer, 1996). At 16 hpf, *shha*, *ptch2* and *smo* mRNAs are expressed in anterior midline neurectoderm (Fig. 2A,D,G). Whereas the expression of *shha* and *ptch2* is very specific, *smo* shows a broader expression throughout the head region. At 28 hpf, *shha* is strongly expressed at the midline (Fig. 2B), whereas *ptch2* is expressed at the midline and strongly in the optic stalk (Fig. 2E) and *smo* shows broad expression throughout the brain and optic stalk (Fig. 2H). At 48 hpf, *shha* midline expression is still strong (Fig. 2C) and all three Hh pathway genes are expressed in RGCs (Fig. 2C,F,I). Thus, Hh pathway components are expressed both during ocular tissue patterning, as well as during RGC axon outgrowth, consistent with a potential role in both processes.

Shha and Smo act non-cell-autonomously in RGC axon pathfinding

We next used cell transplants to test functionally for cell autonomy of Hh pathway components. If Hh signaling directly regulates the guidance of RGC axons, we expect Shha to act non-cell-autonomously, whereas receptor components would act cell autonomously in RGCs. By contrast, if Hh signaling patterns the eye and optic stalk to ensure the correct cellular environment for intraretinal axon pathfinding, we expect both ligand and receptor to act non-cell-autonomously.

We used wt, *shha* and *smo* embryos to transplant retinal precursor cells (RPCs) at 24 hpf from donor into host embryos and analyzed donor RGC axon projections at 54 hpf. To visualize RGC projections, donor embryos carried the *isl2b* transgene (Pittman et al., 2008). When wt RPCs were transplanted into wt hosts, all donor RGC axons exited the host eye through the optic nerve (100% of transplants) (Fig. 3A,H). However, when wt cells were transplanted into *shha* hosts, donor RGC axons were misguided (50% of transplants) (Fig. 3B,H; P=0.015). Similarly, when wt cells were transplanted into *smo* hosts, we found misguided donor RGC axons (62% of transplants) (Fig. 3C,H; P=0.006). When *shha* RPCs were transplanted into wt hosts all donor axons exited the eye normally (Fig. 3D,H), whereas axons were misguided (55% of transplants) when *shha* cells were transplanted into *shha* hosts (Fig. 3E,H; P=0.003). Similarly, donor axons from *smo* into wt transplants always exited the eye normally (Fig. 3G,H), whereas *smo* into *smo* transplants resulted in misguided donor axons (56% of transplants) (Fig. 3G,H; P=0.003). Altogether, we find that wt and mutant RGC axons are equally able to exit the eye in wt hosts but exhibit pathfinding errors when transplanted into *shha* or *smo* embryos. This indicates that both Shha and Smo act non-cell-autonomously in intraretinal axon pathfinding.

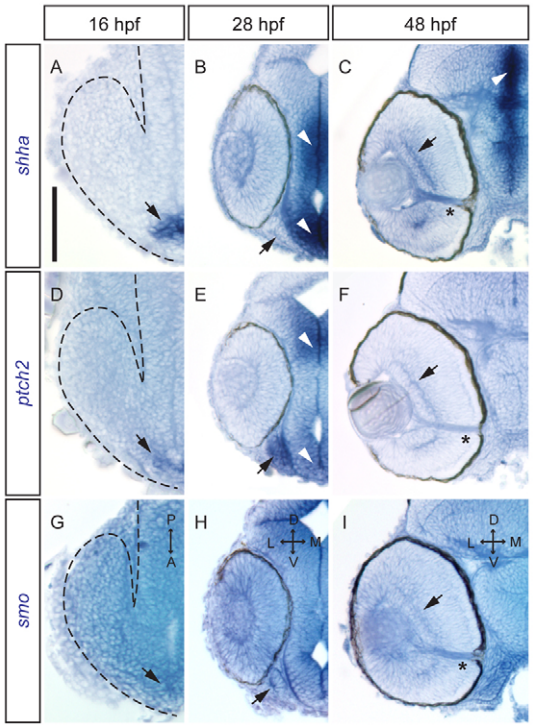

Fig. 2. Hh pathway genes are expressed in the zebrafish optic stalk and RGC layer. Whole-mount in situ hybridizations (15 μm sections) for *shha*, *ptch2* and *smo* mRNA. A,D,G are dorsal views; B,C,E,F,H,I are frontal views. (**A**) 16 hpf, *shha* expression in anterior midline neurectoderm (arrow). (**B**) 28 hpf, *shha* expression at the midline (arrowhead) but not optic stalk (arrow). (**C**) 48 hpf, *shha* strongly expressed at the midline (arrowhead) and in RGC layer (arrow). mRNA also detected in the optic nerve (asterisk). (**D**) 16 hpf, *ptch2* expressed at the anterior midline (arrow). (**E**) 28 hpf, *ptch2* strongly expressed in the optic stalk (arrow) and midline (arrowheads). (**F**) 48 hpf, *ptch2* detected in the RGC layer (arrow) and optic nerve (asterisk). (**G**) 16 hpf, *smo* expressed throughout head region. (**H**) 28 hpf, *smo* broadly expressed, including optic stalk (arrow). (**I**) 48 hpf, *smo* localized in the RGC layer (arrow) and optic nerve (asterisk). Dashed line in A,D,G outlines the optic vesicle. A, anterior; P, posterior; D, dorsal; V, ventral; L, lateral; M, medial. Scale bar: 100 μm.

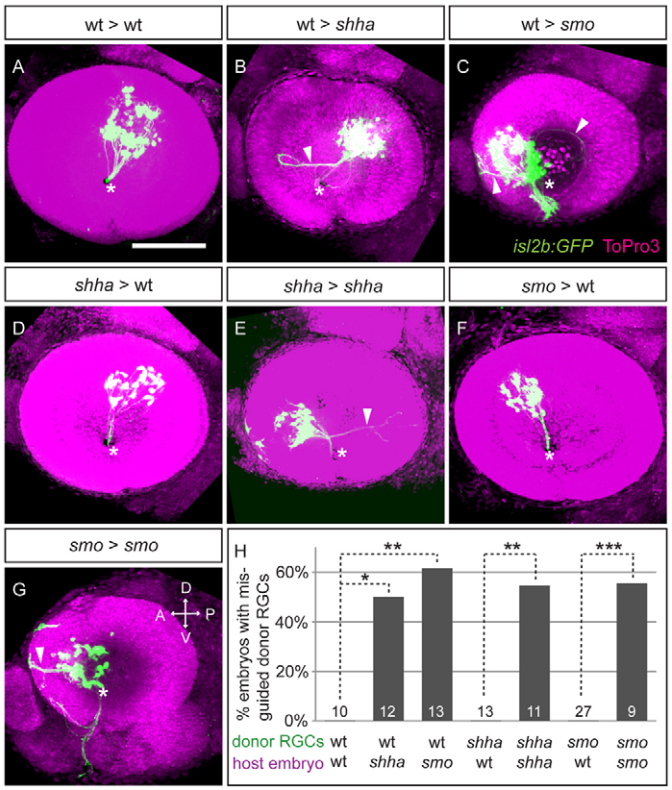

Fig. 3. Shh and Smo act non-cell-autonomously in intraretinal axon pathfinding in zebrafish. (**A-G**) Representative images of host eyes at 54 hpf after cell transplants at 24 hpf. Lateral views of maximum-intensity projections. Wt RGCs axons exit the eye through the optic disc (asterisk) in wt hosts (A), but often misproject (arrowheads) in *shha* (B) and *smo* (C) hosts. *Shha* RGC axons always exit the eye in wt hosts (D), whereas many misproject in *shha* hosts (E). Similar results found with *smo* RGCs in wt (F) or *smo* (G) hosts. Transplanted RGCs are *isl2b:GFP* (*green*) or *isl2b:tagRFP* (pseudocolored green in F,G); nuclei, ToPro3 (magenta). D, dorsal; V, ventral; A, anterior; P, posterior. Scale bar: 100 µm. (**H**) Percentage of embryos with misrouted donor RGC axons. Numbers of embryos shown at base of bars. **P*<0.05, ***P*<0.01, ****P*<0.001, Fisher's exact test.

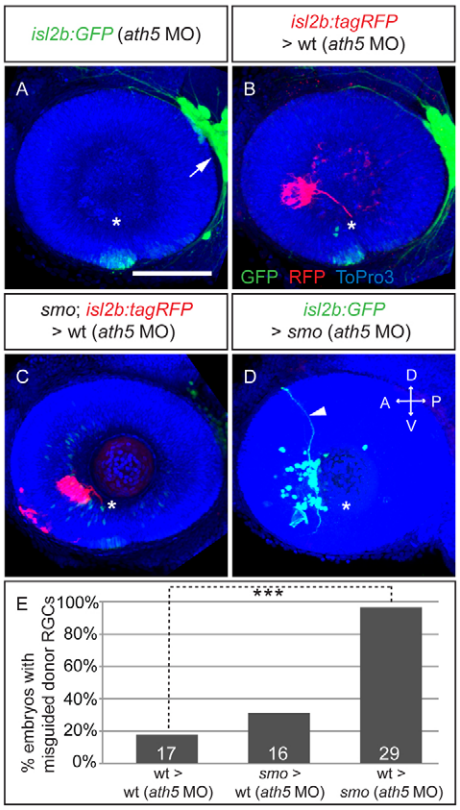

Fig. 4. Transplants into RGC-free hosts confirm non-cell-autonomous effect of Smo in intraretinal axon pathfinding. (**A-D**) Maximum-intensity projections of 54 hpf *isl2b:GFP* or *isl2b:tagRFP* zebrafish embryos injected with *ath5* MO at 1-cell stage (A) and transplanted with donor cells at 24 hpf (B-D). (A) No RGC differentiation in *ath5* morphants; trigeminal ganglion as control for transgene expression (arrow). (B) Wt RGC axons (*isl2b:tagRFP*, red) in *isl2b:GFP* (green) *ath5* morphants rarely make errors. (C) *smo* (*isl2b:tagRFP*) RGC axons in *isl2b:GFP ath5* morphants are rarely misguided. (D) Wt (*isl2b:GFP*) RGC axons in *smo ath5* morphants make errors (arrowhead). Asterisk indicates optic disc. Nuclei, ToPro3 (blue). D, dorsal; V, ventral; A, anterior; P, posterior. Scale bar: 100 µm. (**E**) Percentage of embryos with misrouted axons. Numbers of embryos shown at base of bars. ****P*<0.005, Fisher's exact test.

Previously, we found that pioneer RGCs are necessary to guide later-born axons out of the eye (Pittman et al., 2008). Thus, although we found a non-cell-autonomous effect for Smo, this result could be explained by axon-axon interactions, for which donor RGC axons simply follow host pioneers, thereby masking a cell-autonomous effect of Smo in intraretinal axon guidance. To prevent such pioneer-follower interactions, we inhibited RGC differentiation in host embryos until at least 54 hpf with *ath5* (*atoh7* – Zebrafish Information Network) MO injections. By transplanting donor RGCs into *ath5* morphants, we analyzed axon pathfinding of donor RGCs in a host RGC-free environment. *Isl2b:GFP* embryos were injected with 4 ng *ath5*MO at the 1-cell stage. *Isl2b:tagRFP* donor RPCs were transplanted at 24 hpf into *ath5* morphants and RGC axon projections analyzed at 54 hpf. *Isl2b:GFP* expression in the trigeminal ganglion was used as a control to ensure successful inhibition of RGC differentiation in transgenic embryos (Fig. 4A, arrow). When wt RPCs were transplanted into *ath5* morphants, donor RGC axons exited the eye in most cases; only 18% of the transplants showed intraretinal pathfinding errors (Fig. 4B,E). Similarly, *smo* axons exited the eye in most *ath5* morphants; 31% of the transplants exhibited errors (Fig. 4C,E; *P*=0.44). By contrast, wt RGC axons were misrouted in *smo* mutant *ath5* morphant host eyes in 96% of transplants (Fig. 4D,E; *P*=3.9E-8). These results demonstrate that Smo is required in the environment to ensure correct RGC axon pathfinding, but not in RGCs themselves.

Hh signaling is not required during axon pathfinding for correct axon outgrowth

We used pharmacological inhibition of Hh signaling during embryogenesis to determine when Hh pathway activity is necessary for intraretinal pathfinding. We applied the small molecule compound SANT75 (Smoothened antagonist 75), which specifically inhibits Smo (Yang et al., 2009). We chose SANT75 rather than cyclopamine because of better solubility and stability properties. Because the genes encoding Ptch receptors and Gli transcription factors are themselves target genes of the Hh pathway, expression levels of *ptch2* and *gli1* can be used as readouts for

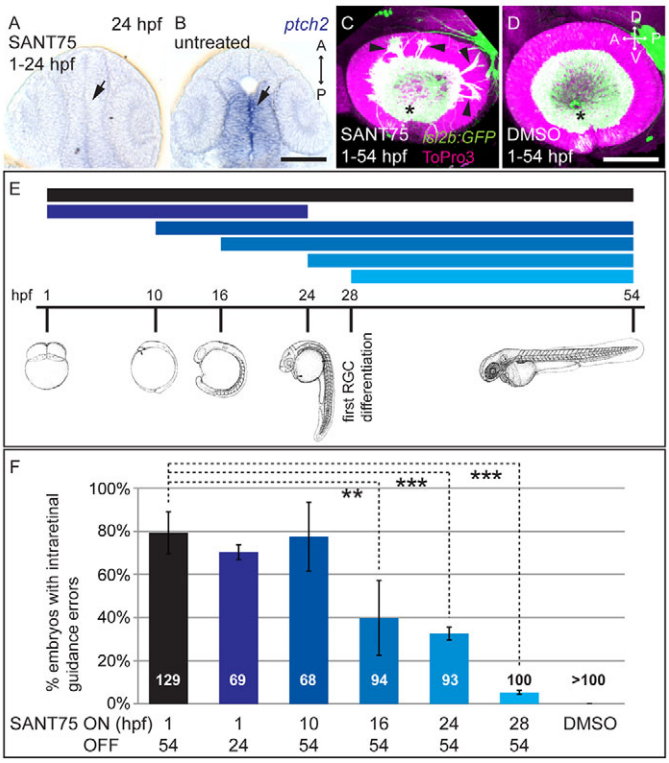

Fig. 5. Shh is required during eye patterning for intraretinal axon pathfinding in zebrafish. SANT75 (40 μM) was bath applied to inhibit Hh signaling for specific stages of embryonic development. (**A**,**B**) Whole-mount in situ hybridizations (15 μm sections), dorsal views. *ptch2* mRNA is expressed at the midline (arrow) in DMSO-treated embryos (24 hpf) (B), whereas expression is lost (arrow) after SANT75 treatment (1-24 hpf) (A). (**C**,**D**) Maximum-intensity projections of lateral views (54 hpf). DMSO (1%) (D) does not affect RGC axon projections in *isl2b:GFP* embryos (green), whereas 40 μM SANT75 (1-54 hpf) (C) yields misguided RGC axons (arrowheads). Nuclei, ToPro3 (magenta); optic disc indicated by asterisk. (**E**,**F**) Different SANT75 application time points (E) and percentage of embryos with resulting intraretinal guidance errors (F). Number of embryos shown at base of bars. Error bars represent s.d. $n \geq 3$ experiments, $^{**}P<0.01$, $^{***}P<0.001$, Student's *t*-test. Line drawings (E) adapted with permission (Kimmel et al., 1995). D, dorsal; V, ventral; A, anterior; P, posterior. Scale bars: 100 μm.

pathway inhibition. SANT75 treatment inhibits *ptch2* and *gli1* expression in a dose-dependent manner (Yang et al., 2009). SANT75 application (40 μM) resulted in downregulation of *ptch2* expression in the brain at 24 hpf (Fig. 5A,B, arrowheads) but no cyclopia. Bath application of 40 μM SANT75 from 1-54 hpf induced a strong intraretinal pathfinding phenotype (79% of *isl2b:GFP* transgenics) (Fig. 5C,F). DMSO-control embryos never showed pathfinding errors (Fig. 5D,F).

At 10 hpf, the eye field is specified and optic vesicle evagination is commencing. At 16 hpf, the optic vesicle is formed but eye patterning is still ongoing. At 24 hpf, basic eye patterning is completed and at 28 hpf, the first RGCs start to differentiate. Applying SANT75 at these specific time points allowed us to determine whether Hh signaling is required before optic vesicle specification (1-10 hpf), for optic vesicle specification and basic eye patterning (10-24 hpf), or during RGC axon outgrowth (after 28 hpf). Treatment with 40 μM SANT75 from 10-54 hpf resulted in 78% of *isl2b:GFP* embryos with intraretinal axon pathfinding errors (Fig. 5F). Similarly, when we started treatment at 1 hpf and washed out SANT75 at 24 hpf, we found intraretinal axon pathfinding errors in 70% of embryos (Fig. 5F). These results are not significantly different from continuous treatment (1-54 hpf), for which 79% of embryos showed errors. Starting treatment at 16 hpf or 24 hpf, by contrast, resulted in significantly fewer embryos with pathfinding errors, 40% (P=0.002) and 33% (P=0.0001), respectively (Fig. 5F). When treatment began at 28 hpf, just as RGCs differentiation begins, only 5% of embryos showed intraretinal pathfinding errors (Fig. 5F; P=4.4E-6). Treatment starting at 1 hpf, 24 hpf and 28 hpf resulted in comparable knockdown of *ptch2* mRNA. Additionally, treatment starting at 1 hpf and 24 hpf resulted in loss of Pax2 expression by 54 hpf, but returned to control Pax2 expression levels by 54 hpf after wash-off at 24 hpf (data not shown). Therefore, the significantly weaker pathfinding phenotype with treatment starting at 24 and 28 hpf indicates that Hh signaling is not necessary at the time of RGC axon pathfinding out of the eye. In addition, our wash-off experiment showed that early inhibition of Hh signaling causes intraretinal pathfinding errors similar to those seen with continuous treatment. Our results show that inhibition of Hh signaling during optic vesicle patterning is sufficient to induce intraretinal axon pathfinding errors later during development.

Optic stalk markers are downregulated in Hh pathway mutants

The strong indication for a role of Hh signaling in eye patterning prompted us to analyze the expression of several optic stalk markers in *shha* and *smo* mutants. Pax2, a transcription factor expressed in the developing optic stalk (Macdonald et al., 1995), was downregulated at 28 hpf in *shha* and lost in *smo* embryos compared with wt (Fig. 6A-C). *netrin 1a*, which encodes a known axon guidance molecule, is expressed along the optic fissure (Macdonald et al., 1997). *netrin 1a* mRNA levels were decreased in *shha* mutants and no expression was found in *smo* eyes at 28 hpf (Fig. 6D-F). *chemokine ligand 12a* (*cxcl12a*, previously known as *sdf1a*) and its homolog *cxcl12b* are expressed in the optic stalk and Cxcl12b was proposed to have an attractive effect on RGC axons inside the eye in zebrafish (Li et al., 2005). *cxcl12a* mRNA levels were strongly downregulated at 28 hpf in the optic stalk in *shha* embryos and not expressed in *smo* mutants (Fig. 6G-I). Thus, loss of Hh signaling leads to downregulation of known transcription factors and axon guidance molecules in the stalk region.

Cxcl12a has an attractive effect on *shha* RGC axons

Our results suggest a model in which Hh signaling during eye specification regulates optic stalk/disc expression of guidance molecules necessary for correct RGC axon pathfinding out of the eye. Although netrin 1 mutants show intraretinal axon guidance errors in mouse (Deiner et al., 1997), we observed no errors using morpholino knockdown in zebrafish (supplementary material Fig. S2). By contrast, zebrafish mutants for *cxcr4b*, a receptor for *cxcl12a*, exhibit intraretinal axon pathfinding errors (Li et al., 2005). Analysis of intraretinal RGC projections in *cxcl12a* mutants revealed the same highly penetrant pathfinding errors (Fig. 7A,B). The intraretinal axon guidance phenotypes in *cxcl12a* and *cxcr4b* mutants are strikingly similar to Hh pathway mutant phenotypes. Therefore, we tested whether downregulation of chemokine signaling at the optic disc in Hh pathway mutants might be responsible for their intraretinal axon pathfinding phenotype. It was reported that Cxcl12b has an attractive effect on RGC axons inside the eye (Li et al., 2005). To determine whether Cxcl12a has a

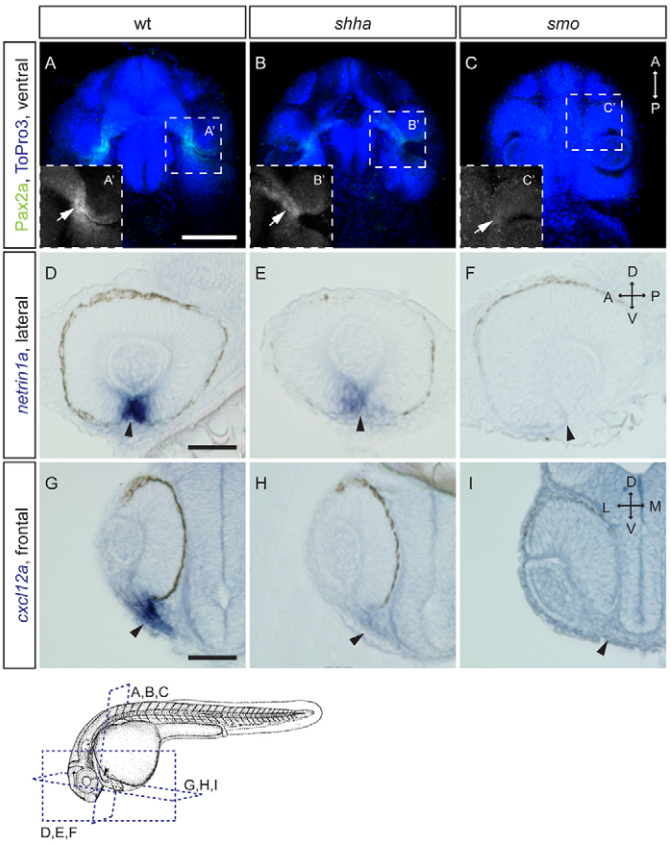

Fig. 6. Expression of optic stalk markers is decreased in Hh mutants. (**A-C′**) Maximum-intensity projections of zebrafish embryos stained for Pax2a (green) by immunohistochemistry (28 hpf); nuclei, ToPro3 (blue). Ventral views. Pax2a reduced in *shha* (B) and absent in *smo* (C) in optic stalk (arrow) compared with wt (A). Insets (A′-C′) show magnified optic stalk region, Pax2a staining only. (**D-F**) Whole-mount in situ hybridizations (15 μm sagittal sections; 28 hpf). *netrin1a* at the optic fissure (arrowheads) is decreased in *shha* (E) and lost in *smo* (F) compared with wt (D). (**G-I**) Coronal sections of whole mount in situ hybridizations (28 hpf). *cxcl12a* expression in optic stalk (arrowheads) is reduced in *shha* (H) and lost in *smo* (I) compared with wt (G). D, dorsal; V, ventral; A, anterior; P, posterior. Illustration below shows plane of views for panels above. Adapted with permission (Kimmel et al., 1995). Scale bars: 100 μm.

similar effect, we induced ectopic *cxcl12a* expression and analyzed whether RGC axons show attraction towards this chemokine. We made an expression construct with the heat-shock promoter driving full-length *cxcl12a* (*hsp70l:cxcl12a-2A-EGFP*). Global overexpression of Cxcl12a after three heat-shocks (at 28, 32 and 36 hpf) led to intraretinal axon guidance errors similar to *cxcl12a* loss of function (Fig. 7D). A control line expressing enhanced green fluorescent protein (EGFP) under the heat-shock promoter did not show any axon guidance errors (Fig. 7C).

To determine whether Cxcl12a has an attractive effect on RGC axons, we transplanted retinal cells from *hsp70l:cxcl12a-2A-EGFP* embryos into the anterior eye of wt or *shha* hosts at 24 hpf and subjected the embryos to three rounds of heat-shock. At 54 hpf, we scored host embryos for anterior axon projection, as indication for an attractive effect of Cxcl12a. Control cells expressing EGFP did not lead to any anterior RGC axon projections (Fig. 7E,I), whereas 22% of wt embryos transplanted with Cxcl12a-expressing cells showed anterior RGC projections (Fig. 7F,I, P=0.04). In 33% of *shha* embryos with anteriorly placed EGFP-expressing cells we observed anterior projections (Fig. 7I), whereas posterior projections were more common in these embryos (Fig. 7G, arrow). Here, anterior and posterior projections represent pathfinding errors due to the loss of *shha* and not due to an attractive effect of EGFP (Fig. 1B; supplementary material Fig. S1). By sharp contrast, Cxcl12a expression in the anterior eye of *shha* mutants led to anterior projections in 100% of transplants (Fig. 7H,I; P=0.0003). These results indicate that Cxcl12a has an attractive effect on RGC axons in both wt and *shha* embryos. In addition, ectopic Cxcl12a expression in *shha* mutant eyes resulted in more embryos with anterior projections than in wt, possibly owing to the decreased endogenous Cxcl12a at the optic disc in *shha* mutants.

The Hh and chemokine pathways interact genetically for intraretinal axon guidance

To investigate further the interaction between the Hh and chemokine pathways for intraretinal axon guidance, we analyzed the axon pathfinding phenotype in *shha* mutants that are either wt or heterozygous for *cxcl12a*. We crossed *shha*/+;*isl2b:GFP* fish to *shha*/+;*cxcl12a*/+;*isl2b:GFP* carriers. At 2 dpf, we scored the intraretinal pathfinding phenotypes and grouped them into four categories: ‘0’, no errors, all axons exit the eye; ‘1’, few errors, most axons leave the eye; ‘2’, most axons make errors inside the eye, few exit; ‘3’, all axons make errors, no axons leave the eye (Fig. 7J). The *shha* and *shha;cxcl12a/+* embryos were separated after genotyping and the severity of the intraretinal axon pathfinding phenotype for both groups was analyzed using Mann-Whitney U statistics. Our analysis showed a significant increase in the severity of the pathfinding phenotype in *shha*;*cxcl12a*/+ embryos compared with *shha* (P=0.001). As *cxcl12a* heterozygous embryos exhibit no intraretinal axon guidance errors, our finding that *cxcl12a* heterozygosity increases the severity of intraretinal axon pathfinding phenotype in *shha* mutants indicates that the Hh and chemokine pathways interact genetically for RGC axon guidance inside the eye.

Chemokine signaling acts directly on RGC axons for correct intraretinal axon guidance

To test whether chemokine signaling has a direct role in RGC axon pathfinding, we performed cell transplants using *cxcr4b* mutants, which lack the receptor for *cxcl12a* in RGCs (Li et al., 2005), as donor or host embryos. Because transplanted RGC axons tend to follow existing axon pathways, we used both unmanipulated and *ath5* morphants that lack RGCs as hosts. Wt cells transplanted into wt embryos exited the eye normally (100% of transplants) (Fig. 8A,G) but when transplanted into *cxcr4b* mutants, transplanted wt cells made errors (66.6% of transplants) (Fig. 8B,G; P=0.003), probably because they followed aberrant axon pathways laid out by earlier born RGCs. Along the same line, *cxcr4b* mutant axons rarely made errors in wt eyes with a full complement of RGCs (15% of transplants) (Fig. 8C,G) but when transplanted into *ath5*MO-injected wt embryos that lack previously formed axon pathways, we observed misguided *cxcr4b* axons in 94.7% of transplants (Fig. 8D,G). Consistently, 33.3% of the transplants exhibited errors when wt cells were transplanted into *ath5* morphants regardless of whether these hosts were wt (Fig. 8E,G; P=0.0014) or *cxcr4b* mutant (Fig. 8F,G). These results show that Cxcr4b acts cell autonomously in RGCs for correct axon pathfinding and supports our hypothesis that chemokine signaling acts directly in intraretinal axon guidance in zebrafish.

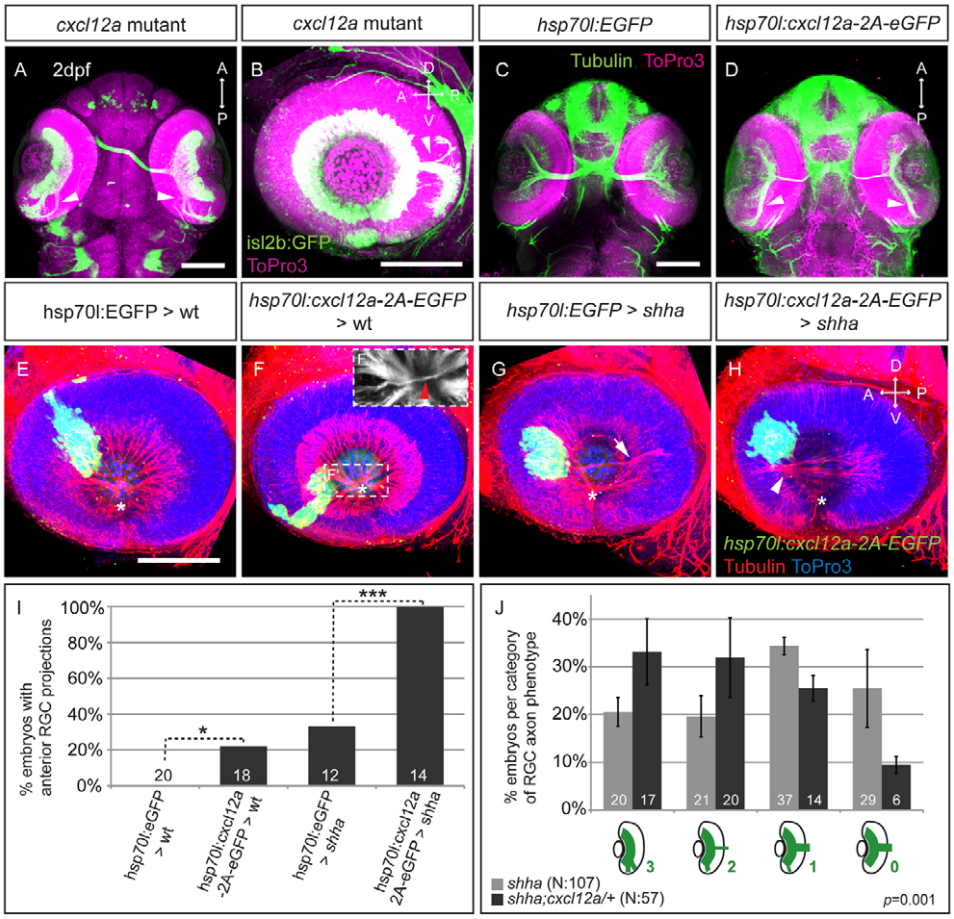

Fig. 7. Cxcl12a acts as an RGC axonal attractant in wt and *shha* and interacts genetically with the Hh pathway in zebrafish. (**A-H**) Maximum-intensity projections of ventral (A,C,D) and lateral (B,E-H) views at 2 dpf. (A,B) *Cxcl12a* mutants exhibit intraretinal axon guidance errors (arrowheads). *Isl2b:GFP* (green); nuclei, ToPro3 (magenta). (C) Normal axonal projections in *hsp70l:EGFP* embryos after heatshock. (D) Global *Cxcl12a-2A-EGFP* overexpression induces intraretinal axon guidance errors (arrowheads). α-tubulin (pseudocolored green); nuclei, ToPro3 (magenta), EGFP not shown. (E-H) Cxcl12a-expressing cells attract RGC axons in wt and *shha* embryos. Transplanted *EGFP*- or *cxcl12a-2A-EGFP*-expressing cells (green), α-tubulin (red); nuclei, ToPro3 (blue). (E) Anterior EGFP-expressing cells in wt embryos do not affect RGC outgrowth. (F) Anterior projections in wt embryos with anterior Cxcl12a-expressing cells. (F′) Substack of boxed region in F with misguided axons (red arrowhead). (G) Rare anterior projections in *shha* embryos with EGFP-expressing cells. (H) *Shha* embryos always show anterior projections with anterior Cxcl12a-expressing cells. Optic disc, asterisk. D, dorsal; V, ventral; A, anterior; P, posterior. Scale bars: 100 μm. (**I**) Percentage of host embryos with anterior RGC projections. Number of embryos shown at base of bars. **P*<0.05, ****P*<0.001, Fisher's exact test. (**J**) Analysis of genetic interaction between *shha* and *cxcl12a*. Percentage of embryos per category (0-3, illustrated below graph) of RGC axon projection phenotype in *shha* (light gray) and *shha;cxcl12a/+* (dark gray). Error bars represent s.e.m. *n*=3 experiments. Mann-Whitney U test, *P*=0.00103, of embryos ranked in four categories in *shha* (*n*=107) and *shha;cxcl12a/+* (*n*=57) populations.

DISCUSSION

Previous research has shown involvement of Shh both in tissue patterning and in direct axon guidance, such as in spinal cord patterning and commissural axon guidance across and along the midline (Ericson et al., 1997; Briscoe and Ericson, 1999; Charron et al., 2003; Bourikas et al., 2005; Okada et al., 2006; Yam et al., 2009; Domanitskaya et al., 2010), as well as in optic stalk and retina patterning and RGC axon guidance along the retinotectal pathway (Ekker et al., 1995; Macdonald et al., 1995; Perron et al., 2003; Trousse et al., 2001; Kolpak et al., 2005; Kolpak et al., 2009; Sánchez-Camacho and Bovolenta, 2008; Fabre et al., 2010; Gordon et al., 2010). We determined that Hh signaling acts non-cell-autonomously for intraretinal axon pathfinding in zebrafish and that Hh pathway activity is required during early eye patterning for correct intraretinal pathfinding later in development. Additionally, we revealed a genetic interaction of the Hh and chemokine signaling pathways for intraretinal axon guidance and showed that Cxcl12a acts as an attractant for RGC axons inside the eye.

Shh regulates optic stalk patterning but not direct RGC axon guidance in zebrafish

Shh expressed by notochord and floorplate cells forms a gradient along the proximodistal axis of the embryo, which is necessary for the specification of optic stalk and retina tissue in both *Xenopus* and zebrafish (Perron et al., 2003; Ekker et al., 1995; Macdonald et al., 1995). High levels of Shh induce Pax2 expression in proximal tissue, whereas distal optic tissue exposed to low levels of Shh expresses Pax6 (Ekker et al., 1995; Macdonald et al., 1995). Overexpression of Shh leads to an expansion of the Pax2-positive

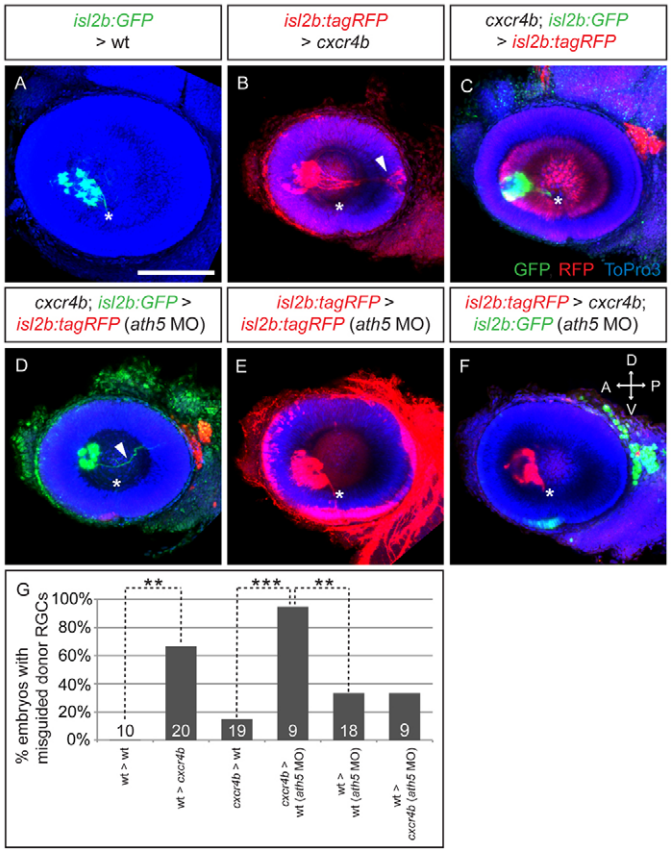

Fig. 8. Cxcr4b acts cell autonomously in RGC for correct intraretinal axon pathfinding. (**A-F**) Maximum-intensity projections of lateral views of 54 hpf zebrafish embryos transplanted with donor cells at 24 hpf. (A) Wt RGC axons (*isl2b:GFP*) in wt embryos exit the eye (asterisk). (B) Wt RGC axons (*isl2b:tagRFP*) often make errors in *cxcr4b* hosts (arrowhead). (C) *cxcr4b* RGC axons (*isl2b:GFP*) exit the eye in most cases when transplanted into wt hosts (*isl2b:tagRFP*). (D) *Cxcr4b* RGC axons (*isl2b:GFP*) are misguided in *ath5* morphants (*isl2b:tagRFP*) in almost all transplants (arrowhead). (E,F) Wt RGC axons (*isl2b:tagRFP*) rarely make errors in *ath5* morphants (*isl2b:tagRFP*) (E)and in *cxcr4b ath5* morphants (*isl2b:GFP*) (F). D, dorsal; V, ventral; A, anterior; P, posterior. Scale bar: 100 μm. (**G**) Percentage of host embryos with misguided donor RGC axons. Number of embryos shown at base of bars. $^{**}P<0.01$, $^{***}P<0.001$, Fisher's exact test.

optic stalk region, whereas loss of midline structures, and consequently of midline-derived Hh signaling, results in an expansion of the Pax6-expressing retinal tissue (Ekker et al., 1995; Macdonald et al., 1995). In our study, we confirmed that loss of Hh signaling in *shha* and *smo* mutants leads to a downregulation of, or loss of, Pax2 expression, respectively, in the zebrafish embryo.

Later in development, murine RGCs express Shh and protein is localized in axons and growth cones as they exit the eye, whereas neuroepithelial cells in the optic nerve express the receptor Ptc (Ptch1 – Mouse Genome Informatics) (Wallace and Raff, 1999; Dakubo et al., 2003). This RGC-derived Hh activity was shown to be required for proliferation and maintenance of the astrocyte population in the optic nerve after basic eye patterning has occurred and axons are leaving the eye (Wallace and Raff, 1999; Dakubo et al., 2003; Dakubo et al., 2008). Although the exact time course of retinal glia development in zebrafish is unclear, we did not detect a role for Hh signaling in intraretinal pathfinding at a corresponding time point.

Hh pathway receptors are also expressed in murine RGCs and ganglion-cell-autonomous Hh signaling has been shown to regulate intraretinal axon guidance in mice (Sánchez-Camacho and Bovolenta, 2008). Similarly, inhibition of Hh signaling using cyclopamine in chick suggested a role for Shh as direct axon guidance molecule for intraretinal pathfinding (Kolpak et al., 2005). Although we detected expression of both Hh pathway ligand and receptors in the RGC layer at the time of axon outgrowth, we showed an RGC-non-autonomous role for Hh signaling in intraretinal axon pathfinding. Instead, we observed a requirement for Hh pathway activity during early eye development for subsequent retinal pathfinding in zebrafish. The early requirement for Hh pathway activity is supported by a previous study, using cyclopamine treatment (Kay et al., 2005). We propose that in zebrafish Hh signaling acts in optic stalk patterning early during eye development but not in direct axon guidance at the time of axon outgrowth to regulate correct intraretinal pathfinding. This role in optic stalk patterning corresponds well with previous findings that Hh signaling regulates axon pathfinding at the zebrafish midline indirectly by determining glial cell position (Barresi et al., 2005). Therefore, although Hh signaling has a conserved role in vertebrate retinal axon pathfinding, the mechanisms appear to be distinct in different model systems.

Axon guidance at the optic disc

In both mouse and zebrafish, Hh pathway mutants show intraretinal axon pathfinding errors where axons fail to turn at the optic disc and instead project within the eye (Sánchez-Camacho and Bovolenta, 2008; Schauerte et al., 1998). Additionally, mouse netrin 1 mutants exhibit intraretinal guidance errors (Deiner et al., 1997). Intraretinal pathfinding errors in a conditional mouse model with loss of *shh* in RGCs have been explained by the lack of netrin 1 expression at the optic disc due to the loss of astrocyte precursor cells in this region (Dakubo et al., 2003). Similar to mouse netrin 1 (Deiner et al., 1997), zebrafish *netrin1a* is expressed in the optic disc/stalk region during RGC axon outgrowth (Park et al., 2005) and we show that loss of Hh signaling leads to downregulation of *netrin1a* expression in the stalk. But in zebrafish, MO-mediated knockdown of *netrin1a* failed to induce any retinal pathfinding errors. None of the other zebrafish *netrin* paralogs is expressed in the eye during development (Park et al., 2005), thus making gene compensation unlikely. We found that the chemokine *cxcl12a* is similarly transcriptionally regulated by Hh signaling. Additionally, *cxcl12a* and *cxcr4b* mutants exhibit intraretinal axon pathfinding errors very similar to Hh mutants. At this point, it cannot be excluded that other guidance molecules affect pathfinding at the optic disc in addition to *cxcl12a*, but the high penetrance of intraretinal axon pathfinding errors in *cxcl12a* and *cxcr4b* mutants as well as our transplants showing a cell-autonomous effect for *cxcr4b* in intraretinal axon guidance support our view of this ligand-receptor pair as a crucial cue at the optic disc in zebrafish. Therefore, we propose that whereas netrin 1 is the main guidance cue inducing turning at the optic disc in mice, this role is taken by *cxcl12a* in zebrafish.

Chemokine signaling in axon guidance

A few studies have implicated chemokine signaling in axon guidance, demonstrating both attractive (Li et al., 2005; Arthur et al., 2009) and repulsive effects (Xiang et al., 2002) of Cxcl12 on axons, as well as a modulatory effect on other guidance cues (Chalasani et al., 2003; Chalasani et al., 2007; Lieberam et al., 2005). In zebrafish, *cxcl12a* is expressed in the distal optic stalk

and MO-mediated knockdown of *cxcl12a* induced intraretinal axon pathfinding errors (Li et al., 2005). Additionally, we showed that *cxcl12a* mutants exhibit a highly penetrant intraretinal axon pathfinding phenotype.

cxcl12b is localized in the proximal stalk region but knockdown of *cxcl12b* alone did not induce intraretinal pathfinding errors (Li et al., 2005). These findings show that *cxcl12a* is necessary for intraretinal axon pathfinding and demonstrate that *cxcl12b* cannot compensate for this role. Previously, it was shown that Cxcl12b misexpression in the eye has an attractive effect on RGC axons (Li et al., 2005). We showed that Cxcl12a exhibits a similar attractive effect on both wt and *shha* mutant RGC axons inside the eye. This demonstrates that Shh is not required as a competence factor for the attractive effect of Cxcl12a. By contrast, we found that *shha* mutant axons showed a stronger attraction towards misexpressed Cxcl12a in the anterior eye compared with wt axons. This could be explained by the stark downregulation of *cxcl12a* in the *shha* mutant optic stalk. Whereas endogenous Cxcl12a at the optic disc attracts wt axons into the stalk, thereby counteracting the effect of misexpressed Cxcl12a in the anterior eye, the low level of endogenous Cxcl12a in *shha* mutants could allow for a stronger attraction of RGC axons towards the misexpressed Cxcl12a.

Genetic interaction between the Hh and chemokine pathways

Hh signaling was shown to promote the expression of chemokine pathway components at the level of *cxcl12* and *cxcr4* in cholangiocyes, endothelial progenitor cells and medulloblastoma (Omenetti et al., 2009; Yamazaki et al., 2008; Yoon et al., 2009). However, the relation between chemokine signaling and the Hh signaling pathway for axon pathfinding was not known. We showed that although *cxcl12a* heterozygosity by itself does not lead to intraretinal pathfinding errors, the loss of one allele of *cxcl12a* in *shha* mutants significantly increases the intraretinal pathfinding phenotype compared with *shha* mutants. Intraretinal pathfinding errors are seen in nearly 100% of *cxcl12a* and *cxcr4b* mutants, whereas Hh pathway mutants only show pathfinding errors in ~50% of the embryos. We observed a low level of *cxcl12a* expression at the optic disc in *shha* mutants, and this residual expression might be sufficient to partly rescue the pathfinding phenotype in *shha* mutants. Using pharmacological Hh pathway inhibition starting at 1 hpf, we induced pathfinding errors in up to 80% of the embryos. This might indicate that maternal *smo* mRNA deposition (Varga et al., 2001) is sufficient to partly rescue optic stalk patterning in *smo* mutants during early eye development even though *cxcl12a* expression was undetectable at 28 hpf in these embryos using in situ hybridization. Therefore, we propose that the increased pathfinding phenotype in *shha* embryos with only one allele of *cxcl12a* compared with *shha* mutants might be explained by a further downregulation of Cxcl12a levels at the optic disc. Decreased levels of *cxcl12a* expression at the disc in *shha* mutants can either be explained by loss of specific gene expression or by a failure of cells differentiation in the optic stalk. Studies in mice showed that Hh signaling is necessary for astrocyte differentiation and maintenance in the optic stalk (Wallace and Raff, 1999; Dakubo et al., 2003; Dakubo et al., 2008). Our genetic interaction experiment, however, supports the model that axon pathfinding errors in *shha* mutants are due to the loss of *cxcl12a*. This identifies the Hh signaling pathway as a regulator of guidance cue expression in the zebrafish optic stalk. A similar indirect requirement for Hh signaling has been observed at the zebrafish chiasm, where Shh regulates the expression of Slit guidance cues at the midline (Barresi et al., 2005).

We were unable to determine whether expression of *cxcl12a* in the optic stalk in *shha* mutants is sufficient to rescue the pathfinding phenotype in these embryos owing to technical limitations. First, polystyrene beads coated with Cxcl12a protein placed into the optic fissure at 24 hpf were pushed out of the eye during optic stalk closure and eye rotation movements. Second, *hsp70l:cxcl12a-2A-GFP* cells transplanted into the fissure could similarly not be detected by 54 hpf. Third, the expression of a *cxcl12a:GFP* construct resulted in GFP expression in the wt optic stalk but this expression could not be detected in *shha* embryos. The lack of transgene expression in mutant optic stalk cells supports our finding of the regulation of *cxcl12a* expression by Hh signaling. Instead, we used cell transplants to show that Cxcr4b acts cell autonomously in RGCs for correct retinal axon pathfinding. This result clearly supports our hypothesis that Cxcl12a expressed at the optic disc acts as direct guidance cue for RGC axon pathfinding inside the retina, in contrast to Hh signaling, which acts indirectly on axon pathfinding through patterning of the eye. It will be interesting to assess whether this mechanism holds true in other organisms also.

Acknowledgements

This manuscript is dedicated to the memory of Chi-Bin Chien. We thank members of the Chien laboratory for discussions and specifically K. M. Kwan and F. E. Poulain for comments on the manuscript. We are especially grateful to M. L. Vetter and R. I. Dorsky for critical reading of the manuscript. We thank Rolf Karlstrom for the *shha* and *smo* mutant fish lines, Holger Knaut for the *cxcl12a* and *cxcr4b* lines, and Shuo Lin for kindly providing the SANT75.

Funding

This work was supported by grants from the National Institutes of Health [RO1 EY12873 to C.-B.C.]; and the University of Utah Interdepartmental Neuroscience Program Achievement Fellowship and the University of Utah Graduate Research Fellowship [to C.S.H.]. Deposited in PMC for release after 12 months.

Competing interests statement

The authors declare no competing financial interests.

Supplementary material

Supplementary material available online at
http://dev.biologists.org/lookup/suppl/doi:10.1242/dev.077594/-/DC1

References

Arthur, A., Shi, S., Zannettino, A. C. W., Fujii, N., Gronthos, S. and Koblar, S. A. (2009). Implanted adult human dental pulp stem cells induce endogenous axon guidance. *Stem Cells* **27**, 2229-2237.

Barresi, M. J. F., Hutson, L. D., Chien, C.-B. and Karlstrom, R. O. (2005). Hedgehog regulated Slit expression determines commissure and glial cell position in the zebrafish forebrain. *Development* **132**, 3643-3656.

Bourikas, D., Pekarik, V., Baeriswyl, T., Grunditz, A., Sadhu, R., Nardó, M. and Stoeckli, E. T. (2005). Sonic hedgehog guides commissural axons along the longitudinal axis of the spinal cord. *Nat. Neurosci.* **8**, 297-304.

Briscoe, J. and Ericson, J. (1999). The specification of neuronal identity by graded Sonic Hedgehog signalling. *Semin. Cell Dev. Biol.* **10**, 353-362.

Chalasani, S. H., Sabelko, K. A., Sunshine, M. J., Littman, D. R. and Raper, J. A. (2003). A chemokine, SDF-1, reduces the effectiveness of multiple axonal repellents and is required for normal axon pathfinding. *J. Neurosci.* **23**, 1360-1371.

Chalasani, S. H., Sabol, A., Xu, H., Gyda, M. A., Rasband, K., Granato, M., Chien, C.-B. and Raper, J. A. (2007). Stromal cell-derived factor-1 antagonizes slit/robo signaling in vivo. *J. Neurosci.* **27**, 973-980.

Charron, F., Stein, E., Jeong, J., McMahon, A. P. and Tessier-Lavigne, M. (2003). The morphogen sonic hedgehog is an axonal chemoattractant that collaborates with netrin-1 in midline axon guidance. *Cell* **113**, 11-23.

Chen, W., Burgess, S. and Hopkins, N. (2001). Analysis of the zebrafish smoothened mutant reveals conserved and divergent functions of hedgehog activity. *Development* **128**, 2385-2396.

Dakubo, G. D., Wang, Y. P., Mazerolle, C., Campsall, K., McMahon, A. P. and Wallace, V. A. (2003). Retinal ganglion cell-derived sonic hedgehog signaling is required for optic disc and stalk neuroepithelial cell development. *Development* **130**, 2967-2980.

Dakubo, G. D., Beug, S. T., Mazerolle, C. J., Thurig, S., Wang, Y. and Wallace, V. A. (2008). Control of glial precursor cell development in the mouse optic nerve by sonic hedgehog from retinal ganglion cells. *Brain Res.* **1228**, 27-42.
Deiner, M. S., Kennedy, T. E., Fazeli, A., Serafini, T., Tessier-Lavigne, M. and Sretavan, D. W. (1997). Netrin-1 and DCC mediate axon guidance locally at the optic disc: loss of function leads to optic nerve hypoplasia. *Neuron* **19**, 575-589.
Domanitskaya, E., Wacker, A., Mauti, O., Baeriswyl, T., Esteve, P., Bovolenta, P. and Stoeckli, E. T. (2010). Sonic hedgehog guides post-crossing commissural axons both directly and indirectly by regulating Wnt activity. *J. Neurosci.* **30**, 11167-11176.
Ekker, S. C., Ungar, A. R., Greenstein, P., von Kessler, D. P., Porter, J. A., Moon, R. T. and Beachy, P. A. (1995). Patterning activities of vertebrate hedgehog proteins in the developing eye and brain. *Curr. Biol.* **5**, 944-955.
Ericson, J, Briscoe, J., Rashbass, P., van Heyningen, V. and Jessell, T. M. (1997). Graded sonic hedgehog signaling and the specification of cell fate in the ventral neural tube. *Cold Spring Harb. Symp. Quant. Biol.* **62**, 451-466.
Fabre, P. J., Shimogori, T. and Charron, F. (2010). Segregation of ipsilateral retinal ganglion cell axons at the optic chiasm requires the Shh receptor Boc. *J. Neurosci.* **30**, 266-275.
Gordon, L., Mansh, M., Kinsman, H. and Morris, A. R. (2010). Xenopus sonic hedgehog guides retinal axons along the optic tract. *Dev. Dyn.* **239**, 2921-2932.
Hammond, K. L., Loynes, H. E., Folarin, A. A., Smith, J. and Whitfield, T. T. (2003). Hedgehog signalling is required for correct anteroposterior patterning of the zebrafish otic vesicle. *Development* **130**, 1403-1417.
Ingham, P. W. and McMahon, A. P. (2001). Hedgehog signaling in animal development: paradigms and principles. *Genes Dev.* **15**, 3059-3087.
Kay, J. N., Link, B. A. and Baier, H. (2005). Staggered cell-intrinsic timing of ath5 expression underlies the wave of ganglion cell neurogenesis in the zebrafish retina. *Development* **132**, 2573-2585.
Kimmel, C. B., Ballard, W. W., Kimmel, S. R., Ullmann, B. and Schilling, T. F. (1995). Stages of embryonic development of the zebrafish. *Dev. Dyn.* **203**, 253-310.
Knaut, H., Werz, C., Geisler, R., The Tübingen 2000 Screen Consortium and Nüsslein-Volhard, C. (2003). A zebrafish homologue of the chemokine receptor Cxcr4 is a germ-cell guidance receptor. *Nature* **421**, 279-282.
Kolpak, A., Zhang, J. and Bao, Z.-Z. (2005). Sonic hedgehog has a dual effect on the growth of retinal ganglion axons depending on its concentration. *J. Neurosci.* **25**, 3432-3441.
Kolpak, A. L., Jiang, J., Guo, D., Standley, C., Bellve, K., Fogarty, K. and Bao, Z.-Z. (2009). Negative guidance factor-induced macropinocytosis in the growth cone plays a critical role in repulsive axon turning. *J. Neurosci.* **29**, 10488-10498.
Kwan, K. M., Fujimoto, E., Grabher, C., Mangum, B. D., Hardy, M. E., Campbell, D. S., Parant, J. M., Yost, H. J., Kanki, J. P. and Chien, C.-B. (2007). The Tol2kit: a multisite gateway-based construction kit for Tol2 transposon transgenesis constructs. *Dev. Dyn.* **236**, 3088-3099.
Laessing, U. and Stuermer, C. A. (1996). Spatiotemporal pattern of retinal ganglion cell differentiation revealed by the expression of neurolin in embryonic zebrafish. *J. Neurobiol.* **29**, 65-74.
Langheinrich, U., Hennen, E., Stott, G. and Vacun, G. (2002). Zebrafish as a model organism for the identification and characterization of drugs and genes affecting p53 signaling. *Curr. Biol.* **12**, 2023-2028.
Li, Q., Shirabe, K., Thisse, C., Thisse, B., Okamoto, H., Masai, I. and Kuwada, J. Y. (2005). Chemokine signaling guides axons within the retina in zebrafish. *J. Neurosci.* **25**, 1711-1717.
Li, Z., Joseph, N. M. and Easter, S. S., Jr (2000). The morphogenesis of the zebrafish eye, including a fate map of the optic vesicle. *Dev. Dyn.* **218**, 175-188.
Lieberam, I., Agalliu, D., Nagasawa, T., Ericson, J. and Jessell, T. M. (2005). A Cxcl12-CXCR4 chemokine signaling pathway defines the initial trajectory of mammalian motor axons. *Neuron* **47**, 667-679.
Macdonald, R., Barth, K. A., Xu, Q., Holder, N., Mikkola, I. and Wilson, S. W. (1995). Midline signalling is required for Pax gene regulation and patterning of the eyes. *Development* **121**, 3267-3278.
Macdonald, R., Scholes, J., Strähle, U., Brennan, C., Holder, N., Brand, M. and Wilson, S. W. (1997). The Pax protein Noi is required for commissural axon pathway formation in the rostral forebrain. *Development* **124**, 2397-2408.
Neumann, C. J. and Nuesslein-Volhard, C. (2000). Patterning of the zebrafish retina by a wave of sonic hedgehog activity. *Science* **289**, 2137-2139.
Okada, A., Charron, F., Morin, S., Shin, D. S., Wong, K., Fabre, P. J., Tessier-Lavigne, M. and McConnell, S. K. (2006). Boc is a receptor for sonic hedgehog in the guidance of commissural axons. *Nature* **444**, 369-373.
Omenetti, A., Syn, W.-K., Jung, Y., Francis, H., Porrello, A., Witek, R. P., Choi, S. S., Yang, L., Mayo, M. J., Gershwin, M. E. et al. (2009). Repair-related activation of hedgehog signaling promotes cholangiocyte chemokine production. *Hepatology* **50**, 518-527.
Park, K. W., Urness, L. D., Senchuk, M. M., Colvin, C. J., Wythe, J. D., Chien, C.-B. and Li, D. Y. (2005). Identification of new netrin family members in zebrafish: developmental expression of netrin 2 and netrin 4. *Dev. Dyn.* **234**, 726-731.
Perron, M., Boy, S., Amato, M. A., Viczian, A., Koebernick, K., Pieler, T. and Harris, W. A. (2003). A novel function for Hedgehog signalling in retinal pigment epithelium differentiation. *Development* **130**, 1565-1577.
Pittman, A. J., Law, M.-Y. and Chien, C.-B. (2008). Pathfinding in a large vertebrate axon tract: isotypic interactions guide retinotectal axons at multiple choice points. *Development* **135**, 2865-2871.
Poulain, F. E., Gaynes, J. A., Stacher Hörndli, C., Law, M.-Y. and Chien, C.-B. (2010). Analyzing retinal axon guidance in zebrafish. *Methods Cell Biol.* **100**, 3-26.
Sánchez-Camacho, C. and Bovolenta, P. (2008). Autonomous and non-autonomous Shh signalling mediate the in vivo growth and guidance of mouse retinal ganglion cell axons. *Development* **135**, 3531-3541.
Schauerte, H. E., van Eeden, F. J., Fricke, C., Odenthal, J., Strähle, U. and Haffter, P. (1998). Sonic hedgehog is not required for the induction of medial floor plate cells in the zebrafish. *Development* **125**, 2983-2993.
Thisse, C. and Thisse, B. (2008). High-resolution in situ hybridization to whole-mount zebrafish embryos. *Nat. Protoc.* **3**, 59-69.
Trousse, F., Martí, E., Gruss, P., Torres, M. and Bovolenta, P. (2001). Control of retinal ganglion cell axon growth: a new role for Sonic hedgehog. *Development* **128**, 3927-3936.
Valentin, G., Haas, P. and Gilmour, D. (2007). The chemokine SDF1a coordinates tissue migration through the spatially restricted activation of Cxcr7 and Cxcr4b. *Curr. Biol.* **17**, 1026-1031.
Varga, Z. M., Amores, A., Lewis, K. E., Yan, Y. L., Postlethwait, J. H., Eisen, J. S. and Westerfield, M. (2001). Zebrafish smoothened functions in ventral neural tube specification and axon tract formation. *Development* **128**, 3497-3509.
Wallace, V. A. and Raff, M. C. (1999). A role for Sonic hedgehog in axon-to-astrocyte signalling in the rodent optic nerve. *Development* **126**, 2901-2909.
Wilson, B. D., Ii, M., Park, K. W., Suli, A., Sorensen, L. K., Larrieu-Lahargue, F., Urness, L. D., Suh, W., Asai, J., Kock, G. A. H. et al. (2006). Netrins promote developmental and therapeutic angiogenesis. *Science* **313**, 640-644.
Xiang, Y., Li, Y., Zhang, Z., Cui, K., Wang, S., Yuan, X.-b., Wu, C.-p. Poo, M.-m. and Duan, S. (2002). Nerve growth cone guidance mediated by G protein-coupled receptors. *Nat. Neurosci.* **5**, 843-848.
Yam, P. T., Langlois, S. D., Morin, S. and Charron, F. (2009). Sonic hedgehog guides axons through a noncanonical, Src-family-kinase-dependent signaling pathway. *Neuron* **62**, 349-362.
Yamazaki, M., Nakamura, K., Mizukami, Y., Ii, M., Sasajima, J., Sugiyama, Y., Nishikawa, T., Nakano, Y., Yanagawa, N., Sato, K. et al. (2008). Sonic hedgehog derived from human pancreatic cancer cells augments angiogenic function of endothelial progenitor cells. *Cancer Sci.* **99**, 1131-1138.
Yang, H., Xiang, J., Wang, N., Zhao, Y., Hyman, J., Li, S., Jiang Jin, Chen, J. K., Yang, Z. and Lin, S. (2009). Converse conformational control of smoothened activity by structurally related small molecules. *J. Biol. Chem.* **284**, 20876-20884.
Yoon, J. W., Gilbertson, R., Iannaccone, S., Iannaccone, P. and Walterhouse, D. (2009). Defining a role for Sonic hedgehog pathway activation in desmoplastic medulloblastoma by identifying GLI1 target genes. *Int. J. Cancer* **124**, 109-119.